Thermographic imaging for early detection of biocolonization on buildings

Stéphanie Eyssautier-Chuine, Kamel Mouhoubi, Fany Reffuveille, Jean-Luc Bodnar

THERMOGRAPHIC IMAGING FOR EARLY DETECTION OF BIOCOLONISATION ON BUILDINGS

Stéphanie Eyssautier-Chuine[a], Kamel Mouhoubi[b], Fany Reffuveille[c] and Jean-Luc Bodnar[b]

[a] Groupe d'Étude sur les Géomatériaux et les Environnements Naturels Anthropiques et Archéologiques EA 3795 – SFR Condorcet FR CNRS ;
3417–2, Esplanade Roland Garros, University of Reims Champagne-Ardenne, Reims, France;
[b] ITheMM - EA 4694, University of Reims Champagne-Ardenne, Reims, France;
[c] Biomatériaux et Inflammation en Site Osseux EA 4691, U.F.R. Pharmacie, University of Reims Champagne- Ardenne, Reims, France

Abstract

Biofilms developed on historical heritage buildings are made of various microbial communities settled and anchored in a substrate. They provide a good medium to the development of macroscopic vegetation which causes irreversible and physical damage to stone structure. Infrared thermography (IRT) measurements have been performed in laboratory scale to investigate the applicability of this non-destructive technique to an early detection of microbial biofilms on stone surface. Detecting biofilms before stone soiling is important in Cultural Heritage conservation to avoid both irreversible damage and building restoration costs.

Active IRT was set up on a French limestone used in many French buildings and monuments. Samples were collected after six-months of exposure in an outdoor biofouling test during which they were colonized by microbial biofilms. They have been compared with controls with no biofilm. Experimental set-up has been carried out in dry and damp conditions to simulate different climatic conditions. First results displayed a different thermal response: stone surfaces with biofilm reached higher temperatures and they cooled down faster than row stones. Biofilm entailed a change of the stone thermal behaviour similar to a monolayer. IRT detected biofilm with a better efficiency in dry than in damp condition.

Keywords: Infrared thermography, detection, biofilm, stone building

Introduction

Natural stone has been used for its durability to raise buildings throughout the ages. Its longlasting renown has been disputed since the 20th century. The industrial revolution generated environmental pollution which did not exist previously and hastened the ageing and the degradation of buildings and monuments. Public authorities have become aware of Cultural Heritage weakness through the environmental changes. In temperate climates, colonisation of buildings by micro-organisms (called biocolonisation) contributes to their degradation and is a considerable problem for their maintenance. It is firstly a driving factor for the aesthetic aspect of building walls (Tran et al., 2014; Pozo-Antonio et al., 2017; Santunione et al., 2019). Microbial communities composing biofilms spread thanks to nutritive elements found in the components of stone, and favour the anchorage of other micro-organisms such as fungi, algae, moss and lichen (McNamara & Mitchell, 2005; Warscheid & Braams, 2000). Over time, biofilms induce an undesired change of stone properties through biochemical action made by the cell's metabolism, which causes a mineral dissolution (Li et al., 2008). Moreover, such a mechanical damage plays a significant role in this irreversible weathering caused by the lichen hyphae penetration, weakening the stone until it breaks (Ahmed & Holmström, 2015; Nuhoglu et al., 2006; Papida et al., 2000; Pinheiro et al., 2018). Consequently, restoration may induce significant costs due to cleaning and changing building materials to avoid definitive losses of heritage.

In this respect, the early biofilm growth on stone walls must be taken into account to limit financial damages; The colour measurement is a usual non-destructive technique employed in building restoration. This method assesses the biological growth spread on stone - which has different colours - and consequently the weathering of building walls. (Grossi et al., 2007; Borderie et al., 2014; Eyssautier-Chuine et al., 2014). Other factors inducing colour variations are not induced by micro-organisms, such as moisture, urban pollution and the natural ageing of the stone patina. Accordingly, an earlier detection of biocolonisation should be more profitable than a visual one.

In this study, infrared thermography (IRT) has been investigated in first assays in order to assess the sensitivity of this non-destructive technique to track down the biocolonization earlier than colourimetry. It is an evaluation tool commonly used in monitoring and maintenance of buildings and works of art studies. The substrates surface and subsurface are tested by analysis of thermal emissions. It is a powerful technique for art analysis thanks to its non-contact imaging application and its earliness to detect many flaws before visual detection (Bodnar et al., 2012; Gavrilov et al., 2014; Mouhoubi, 2016). This military-origin technique (detection of missile launches, 1960s) has been developed in the field of civil research in the 1980s due to more affordable camera prices (Carlomagno & de Luca, 1987; Maldague, 2001; Vavilov & Maldague, 1992) and has since led to successful developments in many fields (engineering, medicine, industry). The applicability of IRT in Cultural Heritage investigates a wide range of issues such as tracking cracks in paintings, diagnostics of buildings damage by moisture and performance of treatments for consolidation on porous stones and restoration of masonries (Avdelidis & Moropoulou, 2004; Moropoulou et al., 2013). IRT has already been applied to measure the heat released by lichens on outer walls and in soils (Garty, 1990; Kluge et al., 2013).

This work analysed thermal responses of biocolonised stones after stimulation by a heating pulse (active IRT). Natural stone samples have been previously exposed six months in a garden where biofilms grew, then compared to non-exposed samples. The experiment has been set up in a laboratory condition in order to avoid external artefacts and to optimize the protocol. Thermal responses have been monitored on dry and damp stones to come closer to natural weather conditions. Beside, water is a significant parameter for the biofilm growth and changes the thermal behaviour of building materials (Barreira & Almeida, 2015; Moropoulou et al., 2018).

Short overview on scientifical techniques of biodeterioration study on monuments

The biodeterioration of buildings was more seriously considered in Europe since the eighties due to lower air pollution imposed by environmental rules, decreasing sulphur concentration and therefore favouring deposition of organic compounds (Grossi & Brimblecombe, 2008). A large range of techniques are used to identify microbial species and analyse their physiological activity on stone to better understand the process leading to the stone weathering. Biofilms on stone are composed of biological microcolonies embedded in an organic polymer matrix, they also hold various microbial species which have physiological activities (Di Martino, 2016). Many techniques are used to quantify and describe them and to understand their function on the weathering process of stone (Hirsch et al.,

1995; Mihajlovski et al., 2014). Destructive techniques of collecting contaminated stone samples are used in situ by detaching, crushing and drilling, while non-destructive techniques collect biofilms by scraping, swab using and cutting. Biofilms are observed by diverse microbiological analyses, such as scanning electron microscopy (SEM), wet-mode environmental scanning electron microscopy (ESEM) and transmission electron microscopy (TEM). Morphological information of biofilm are provided as well as its interaction with the stone surface. Molecular techniques like high-throughput genetic analysis (16S rRNA and 18S rDNA gene sequencing, metagenome analysis) are currently used to study the phylogenetic diversity of the microbial communities. Technological advances contributed to the development of several in-site microscopy techniques to study biofilm-stone relationship using a SEM in back-scattered mode (SEM-BSE), low-temperature SEM (LTSEM) and confocal scanning laser microscopy (CSLM) (De los Rios & Ascaso, 2005). Nonetheless, these microscopic techniques require expensive devices and a considerable experience which local authorities and restorers cannot apply on all the built heritage. Consequently, colourimetry is a common and rapid technique used on site to monitor changes of stone surface appearance due to the expanding biological colonisation of walls (Cutler et al., 2013; Gambino et al., 2019) and to evaluate the efficiency of biocide treatments (Becerra et al., 2020; Goffredo et al., 2017). Nevertheless, colourimetry provides a limited expertise to detect biofilm growth since colour variations of built heritage can be induced by many factors independent of biocolonization.

Materials and methods

Substrate and biofouling test

Savonnieres stone has been chosen for its renown and its wide use in major buildings and monuments in Northern France and Western Europe from the antiquity to 19^{th} - 20^{th} centuries, as well as part of monument restorations. It is a clear grey limestone made of oolit vacuolar grains and shell debris (Figure 1) and dated from Lower Tithonian (150 My). The texture is grain-supported and composed of intragranular moulding macropores by dissolution of oolit nuclei. Savonnieres stone is still mined in the two last quarries in the vicinity of Saint Dizier city in the East of France. Its petrophysical properties have been conducted, for the evaluation of the water transfer inside the stone which is a significant parameter for the micro-organisms growth.

The porosity characterization has been carried out by the mercury (Hg) intrusion porosimeter (Micromeritics Autopore IV 9500): pressure reached 247 MPa and pore radii sizes were 0.003-178 µm. Savionnieres stone has a high porosity (40.4 %) and is composed of more than 58 % of pores of large size access radii (> 1 µm) located inside the grain, 29 % of pores in the medium size range radii (1-0.1 µm) and finally 13 % of pores in the small range radii (0.1-0.01 µm) located between grains as a partial cementation of the stone. The capillary coefficient has been assessed by the capillary absorption test (European Commitee for Standardization, 2010). The stone has a high coefficient of 38.1 $g.m^{-2}.s^{-1/2}$, suggesting a fast water absorption due to a good connection between pores (Table 1).

A biofouling test has been set up with the aim of ageing stone samples with the micro-organisms growth on them. It was located in Rheims city, more precisely inside the garden of Sacré Coeur secondary school which had limited access to people and many trees favour the stimulation of biocolonisation on stones. Samples (2 x 2 x 1 cm dimension) have been settled on a galvanized steel platform, 1 m above the ground and 20° tilted to the SW to limit water stagnation and allow as much daylight on them as possible. They were collected at six months of ageing and conditioned at room temperature. One batch of three replicates was damped in a container with water on the bottom to insure saturation and a second one has been kept dry for the IRT experiment. Other triplicates have been collected every two months to cultivate bacteria on growth media in laboratory. Four bigger samples (10 x10 x 5 cm dimension) have been exposed to measure the colour variation of stone surface.

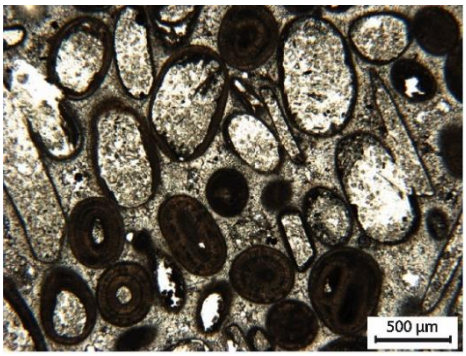

Figure 1 : Savonnieres stone is an oolitic grainstone with a microporosity inside oolit nuclei and a microporosity in the spar cement between grains (thin section and polarized light)

Stone name	Savonnieres
Classification (Dunham)	Grainstone
Water absorption coefficient C1 ($g.m^{-2}.s^{-1/2}$)	38.1 ± 4.4
Water porosity (%)	40.4 ± 2.0
Pores (%) > 1 µm	58.0 ± 3.0
1 > pores (%) > 0.1 µm	29.0 ± 3.0
0.1 > pores (%) > 0.01 µm	13.0 ± 4.0

Table 1: Description and characteristics of Savonnieres stone

Detection of bacteria growth on stones

Samples from the outdoor ageing station have been cleaned up and immersed in a PBS (Phosphate Buffered Saline) buffer solution. Then bacteria have been extracted from stones thanks to ultrasound (40 kHz) for a duration of 5 minutes and cultivated for the ones having the ability to grow in nutrient agar-agar plates. The growing bacteria cannot provide quantitative information of development on stone since only 1 % of micro-organisms is readily cultivated in vitro, with the majority of all bacteria remaining 'unculturable' using standard methods (Vartoukian et al., 2010). Nevertheless, the cultivation of bacteria provides a proof of their presence despite the lack of colour on stones.
In addition, the biological colonisation has been observed in environmental SEM (Hitachi TM-3030 plus Tabletop Microscope) in order to analyse the settlement according to the stone texture. Outdoor samples were entirely introduced into the microscope chamber and were placed on a double-sided adhesive carbon tape. The accelerating voltage for imaging was 15 kV at a working distance of 6 mm. All images were acquired in the back-scattered electron mode.

Detection of biofilm by colourimetry

Colour measurements have been carried out on four samples of 10 x10 x 5 cm dimension from five to twelve months of exposure. They have been performed with a Chroma Meter CR-400 from Konica-Minolta with a light projection tube CR-A33c of 11 mm diameter (corresponding to the measurement zone). Calibrations were performed with a white ceramic plate CR-A43. Values are given in the CIE-$L^*a^*b^*$ colour space (European commitee for Standardization, 2008). Three dimensionless parameters determine the colour location in colour space: L^* indicates lightness; a^* and b^* are the chromaticity coordinates. The global colour variation (ΔE) was calculated from the following formula:

$$\Delta E_{ab} = \sqrt{\Delta L^{*2} + \Delta a^{*2} + \Delta b^{*2}} \quad (1)$$

where ΔL^*, Δa^* and Δb^* were the differences between the measurements on stones before exposure and after 5 to 12 months' exposure. The average has been calculated from 25 measurements for each sample surface.

Active IRT

Theoretical model of the flash pulse

The flash pulse is an experimental protocol used extensively in IRT (Jaeger & Carslaw, 1959; Özışık, 1993) thanks to its ease of use, and the direct access to the pulse response which is the key characteristic of the material. Moreover, the theoretical model provides easy and short calculations. It uses a plane, parallelepipedal, laterally semi-infinite (in x and y) and adiabatic (no convection on all faces) sample with L thickness. It is excited on the front face, in x = L by a pulse of surface Dirac Q.δ (t) (Figure 2). Initially the sample is in thermal equilibrium with the environment at 0 ° C temperature.

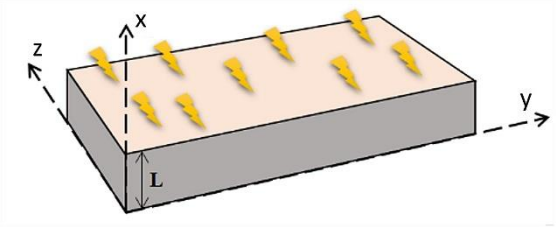

Figure 2 : Sample subjected to a surface Dirac (Mouhoubi K., 2016)

The differential system to be solved is as the following (2):

$$\begin{cases} \dfrac{\partial^2 T}{\partial x^2} - \dfrac{1}{a}\dfrac{\partial T}{\partial t} = -\dfrac{P(x,t)}{\lambda} \\ \left.\dfrac{\partial T}{\partial x}\right|_{x=0} = 0 \quad \text{en x=0, pour t>0} \\ \left.\dfrac{\partial T}{\partial x}\right|_{x=L} = 0 \quad \text{en x=L, pour t>0} \\ T(x,0) = 0 \end{cases} \tag{2}$$

Where T is the temperature (K), t is time (s), x is a spatial coordinate (m), P(x, t) is the internal volumic power depending on x and t (W/m^3), λ is the thermal conductivity (W/m.K), L is the sample thickness (m) and *a* is the thermal diffusivity (m^2/s)

The resolution of this global system refers to Green's formalism (Beck et al., 1992) which consists in finding a solution to the previous homogeneous differential system and then in using function libraries that take into account the geometrical configuration of the experiment. Calculations from the formula (3) lead to the front surface temperature versus time:

$$T(L,t) = \frac{Q}{\rho C_p L}\left(1 + 2\sum_{m=1}^{\infty} \exp\left[-\frac{m^2\pi^2 at}{L^2}\right]\right) \tag{3}$$

where Q is the total heating energy applied to the material (cal/cm^2), C_p is the thermal capacity (J/kg m3), ρ is the density (kg/m3) and m is the serial order.

The study at the function limits leads to the simplified formula of the temperature field on the front surface (4):

$$T(t) = \frac{\alpha . Q}{b\sqrt{\pi t}} \tag{4}$$

where α is the absorptivity of the material (between 0 and 1), b is the thermal effusivity combining density (ρ), thermal conductivity (k) and specific heat (c) such as: $b = \sqrt{\rho k c}$

From this formula and in the case of a homogeneous and semi-infinite material, the temperature decreases progressively over time from the $\mathrm{Log}(T(t)) = \frac{1}{\sqrt{t}}$ function which follows a -1/2 slope regression line in a Log-Log graphical representation. In consequence, when the cooling kinetics is represented by a noticeable slope break different than the -1/2 slope line, the material is not homogeneous and highlights defaults inside it.

In an experiment, the flash method is set up to investigate a material subjected to a very short thermal pulse (extended flash, few milliseconds), equivalent to a "Dirac" pulse. The material is heat-affected and a part of energy is absorbed. The gain depended on the physical and chemical properties of the material. After the pulse, the cooling of the material emits infrared radiation. A thermographic camera records the thermal diffusivity on the material by the curve describing temperature versus time (Kylili

et al., 2014). This approach attempted to compare the thermal behaviour of a material as stone in both conditions, at the early stage of the biofilm growth at the surface and without biofilm.

Experimental setting

In the experiment of biofilm detection, a ring lamp of 20 cm diameter emitted an optical flash releasing 3000 J for 5ms. The absorption of photons increased the temperature in the vicinity of the lighted area comprising the sample surface. A bolometer camera (FLIR SC655) recorded the thermal effect as a response of the light excitation in long wave infrared (8-12 µm) with a temperature ranging from - 40 - 150°C. The thermal response has been recorded for 5 s and the acquisition frequency was 50 Hz. It started by a maximal temperature rise and a progressive decrease in the temperature due to the heat diffusion into the material.

IR experiment has been carried out on batches of three stones, one batch is colonized by a natural biofilm and compared to a control batch without biofilm which has not been aged and has been sterilized to not induce bacteria (Figure 3). Moreover, two other batches with biofilm and control have been assessed in the damp conditions too. Samples have been water-saturated in the interests of comparing thermal signals as moisture is a parameter which occurs in outdoor conditions and alters substrate temperature (Moropoulou et al., 2014; Zhang et al., 2018).

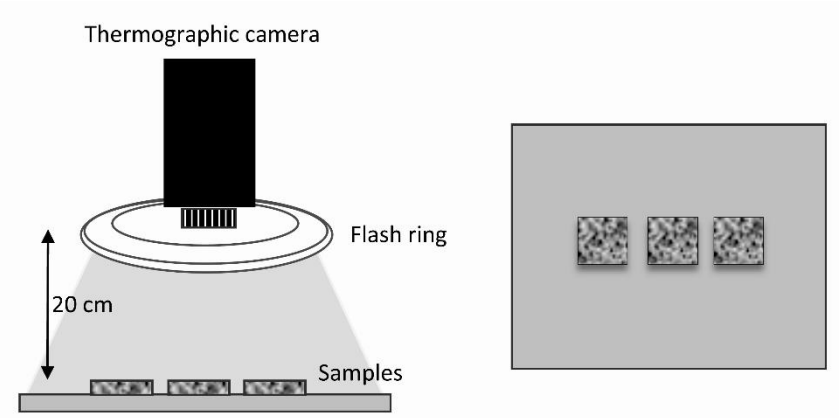

Figure 3: Schematic sketch of experimental setup with IR system

Results

Detection of biofilm on stones by laboratory culture and SEM observations

The bacterial culture on agar-agar medium showed that bacteria appeared from the three replicate samples at two months' exposure time and three different bacterial species have been visually noticed, red, orange and beige. Bacteria continue to develop afterwards (Figure 4). Accordingly, at six months' exposure time, micro-organisms have already colonized the stones.

Biofilms have been observed in environmental SEM, they revealed different species growing on the stone surface showing dark grey patches of embedded cyanobacteria (indeterminate) in EPS (extracellular polymeric substances). They are located firstly in the microporosity between microspar crystals of calcite composing the matrix and on the nuclei of oolit grains that have not been dissolved. The microbial development can be limited inside the grains by the oolitic cortex as a calcitic fringe (Figure 5(a)). When the nuclei of grains have been dissolved creating big macropores, the stagnation and the low evaporation of water inside them raised the biofilm development with algal filaments (Figure 5b). Moreover, cyanobacteria could be observed in dark grey colour between stone crystals being in light grey (Figure 5(c,d)). Accordingly, the texture and the pore network of the stone allowed the spreading of biofilm thanks to a high porosity and well connected large pores which increased the water flow into the stone, therefore a supply to micro-organisms.

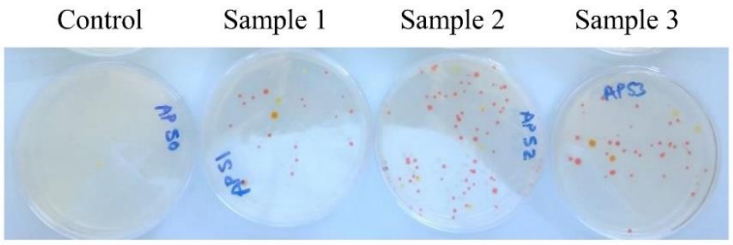

Figure 4 : Bacterial growth in agar-agar plates from three stone samples and control.

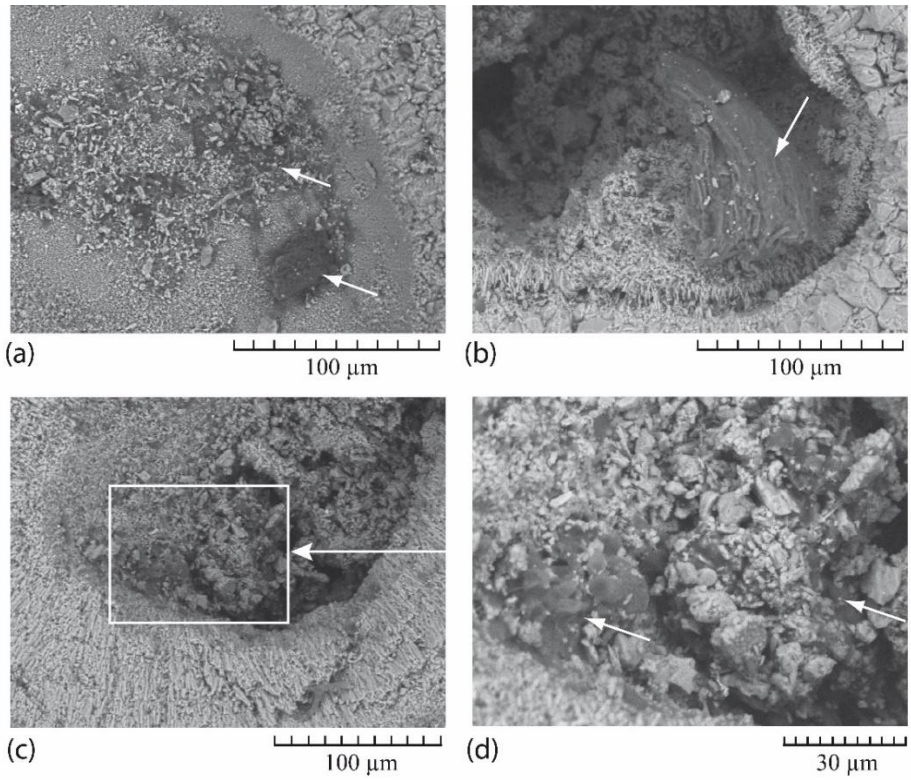

Figure 5: SEM images of microbial communities on Savonnières stone. (a) Biofilm anchored in the microporosity on an oolit nucleus. (b) Algae developed inside the macroporosity. (c) and (d) cyanobacteria growth inside a macropore.

Detection of biofilm on stones by colourimetry

At five months of exposure time, ΔE varied from 1.3 and 1.7. The low values indicated that stone colour at five months of exposure was very close to the natural stone colour at the beginning of the experiment (Figure 6). At six months of exposure, ΔE ranged between 0.9 and 1, the colour parameter did not detect the biofilm growth on stones despite the previous results obtained from SEM observations and the bacterial growth on medium which revealed the micro-organisms occurrence. ΔE were similar until eight months of exposure time at least. Then at 11 months, ΔE increased significantly (from 1.9 to 5.2) and the higher variability of data (from 0.6 to 1.3) showed an inhomogeneous colour on stones due to the biocolonization. Finally, at twelve months, ΔE continue to increase even higher than previously (from 4.2 to 7.9 with a standard deviation from 1.0 to 1.7) and evidenced the biological settlement on samples.

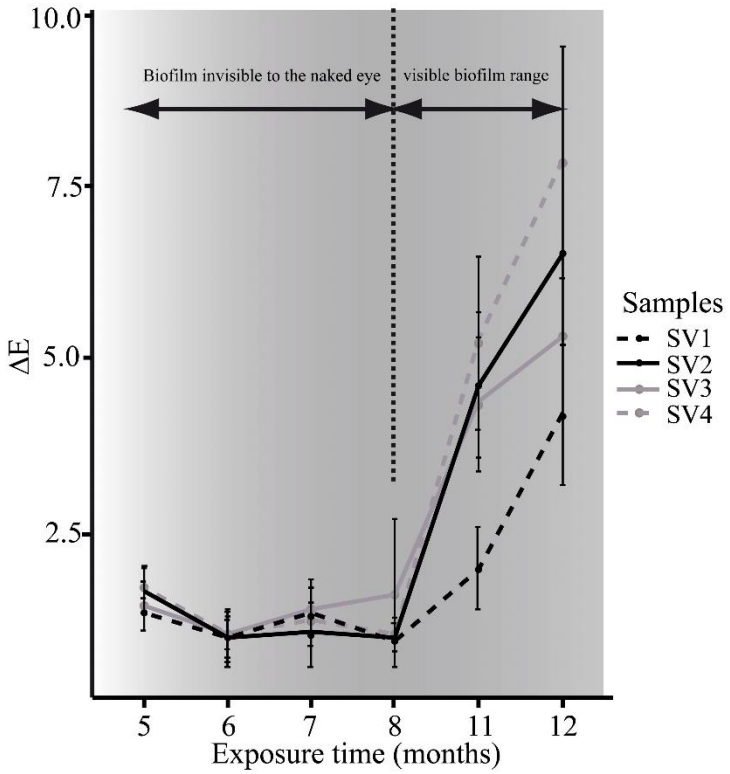

Figure 6 : Global variation ΔE represents the difference of colour between the stone surface before exposure and at different months of exposure for four stone samples (SV1-SV2-SV3-SV4).

Detection of biofilm by IRT

The temperature of the stone surface has been measured from thermographs recorded by IR Explorer® software. Temperature variations (ΔT) have been calculated between the temperature before the flash pulse and the temperature after it. Considering the low deviation standards ranging from 0.01 to 0.07 K, data from stones of each batch were homogeneous and ΔT have been averaged. Figure 7(a) reported the average of ΔT versus time in dry condition. Maximum temperature reached 4.50 K for stones with biofilm and 3.2 K for controls. Thus the maximum heating was higher on stone surfaces with biofilm than on raw surfaces. At 0.20 s, both curves converge at 2.15 K, then ΔT from stones with biofilm were lower than ΔT of controls until the end of the experiment. Moreover, calculation of the cooling time at 60 % from maximum temperature (T max) for each sample displayed a cooling time from 0.26 to 0.34 s for stones with biofilms and 0.80 to 1.06 s for control stones (Figure 7(b)). The cooling time of stone surfaces was faster when they have a biofilm than without it.

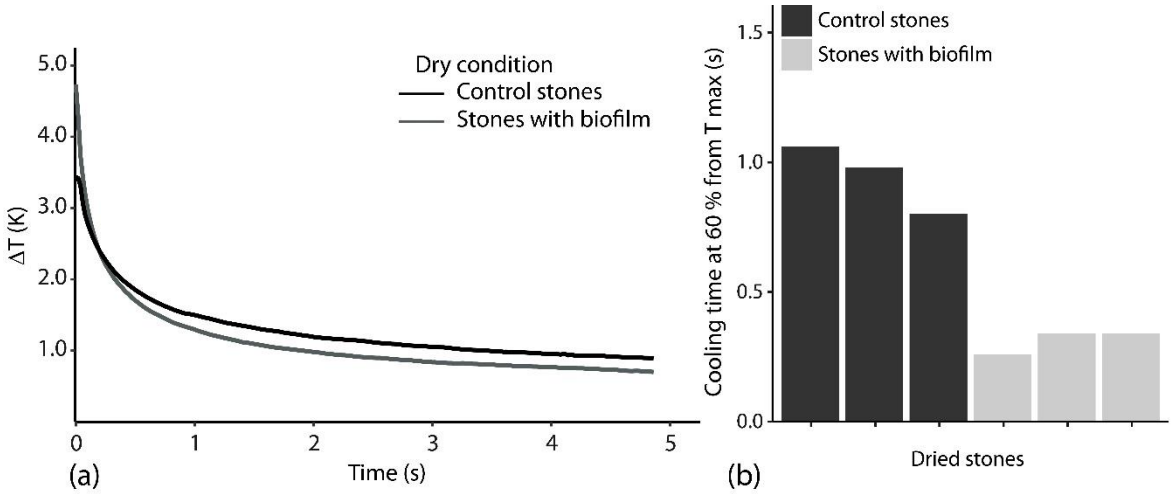

Figure 7: (a) Temperature variation (ΔT) over time after a flash pulse at the surface of dried stones without biofilm (black color) and with biofilm (grey color). (b) Cooling time reached at 60 % of maximum temperature.

In damp condition, results displayed a maximum temperature reaching 2.80 K for stones with biofilm and 2.50 K for controls. Thus, maximum heating was higher for stones with biofilm (Figure 8(a)). At 0.16 s, ΔT of both batches decreased at 1.90 K, then biofilm stones ΔT were lower.
The comparison of the cooling time at 60 % from T max disclosed a cooling between 0.66 s to 0.72 s for stones with biofilm and 1.18 s to 1.53 s for control stones (Figure 8(b)). Consequently, the biofilm at the stone surface hastened the cooling.

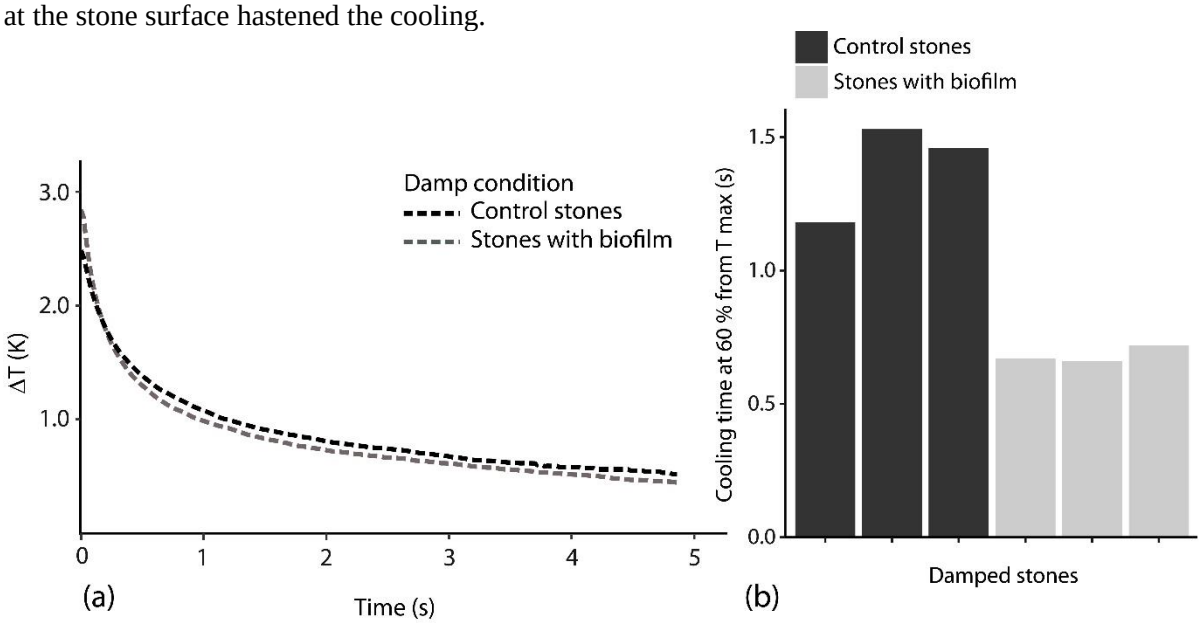

Figure 8: (a) Temperature variation (ΔT) over time after a flash pulse at the surface of damped stones without biofilm (black color) and with biofilm (grey color). (b) Cooling time reached at 60 % of maximum temperature.

The cooling kinetics has been plotted in a Log-Log scale. Data before 0.10 s couldn't be considered, the non-linear line of the detection chain was an artefact due to a recording too close to the pulse phase. The temperature decrease was linear for every stone through time. The slope of the regression line has been compared to the -1/2 slope line of the $1/\sqrt{Time}$ function which is significant of a thermal response to a homogeneous material. This -1/2 slope line is regarded as the reference.
In dry condition, the controls slope of the regression line (-0.37) was lower than the reference (Figure 9(a)), which meant that Savonnieres stone did not have a homogeneous material thermal behaviour. Regarding stones with biofilm, the slope of their regression line (-0.48) was very close to the

reference (Figure 9(b)), they had therefore a thermal response which fit to a homogeneous material one. The biofilm on the surface obviously changed the thermal behaviour of the stone.
In damp condition, the controls slope of the regression line was also lower (-0.40) but it tended towards reference (Figure 9(c)). The cooling kinetics of stones with biofilm had a slope close to the reference as well (-0.47) (Figure 9(d)). The water inside the stone therefore modified the thermal behaviour which tended to a homogeneity of the material.

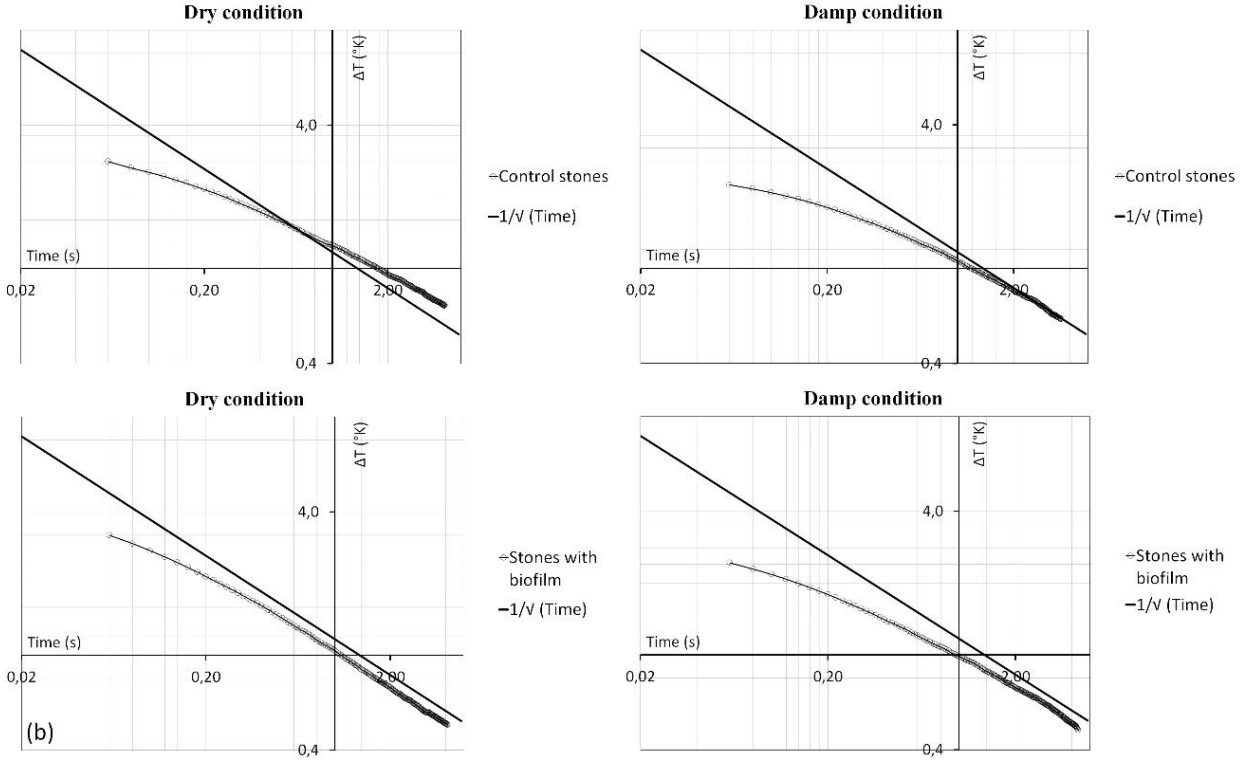

Figure 9: Graphs describing temperature variations (ΔT) at the stone surface versus time after the flash pulse in Log-Log scale for controls (a) and stones with biofilm (b) in dry condition and for controls (c) and stones with biofilm (d) in damp condition. Curves have been compared to the function ($1/\sqrt{Time}$) reflecting a homogeneous and semi-infinite material (black line).

Discussion

IRT tests on the Savonnieres limestone displayed that after the light excitation, the kinetics of heating and cooling were modified when biofilm developed.
Considering the stones with biofilm, in both conditions, the maximum temperatures were higher and the cooling was faster. Moreover, all the temperatures values were higher in dry condition for stones with biofilm or not. The temperature evolution depends on several parameters as described in formula (4), it is related to the absorptivity (α) which is a radiative property and defines the ability of the material to absorb the energy flow. Considering $\alpha_{limestone}$ is 0.6 and α_{eau} is 0.08 in the spectral bands of excitation (visible range) (De Vriendt, 1998) and considering that Savonnieres stone is made of macropores properties and has a high water porosity (40.4 %) (Table 1), water plays a significant role on the absorptivity of the material and consequently on the heating of the surface. This confirmed previous studies in which authors explained that areas affected by water present lower temperatures (Avdelidis et al., 2003; Moropoulou et al., 2018). Biofilm modifies the stone absorptivity and the use of IRT confirmed it.
For control samples in dry condition, the temperature versus time in Log-Log graph highlighted a deviation from the reference. Savonnieres stone is not a thermally homogeneous material due to the significant air amount in the porosity causing thermal discontinuities. Given that effusivity (*b*) is the ability of a material to respond to a thermal disturbance, it is assessed that temperature is inversely related to *b* (formula (4)). Dry limestone and a high air amount inside have different effusivities: $b_{limestone}$ is 1509.0 $J.K^{-1}.m^{-2}.s^{-1/2}$ while b_{air} is 5.4 $J.K^{-1}.m^{-2}.s^{-1/2}$ (Hladik, 1997). Air acted as a heat isolator and

decreased the energy propagation into the stone which explained that dry stones were not thermally homogeneous. Contrary to control stones, the regression line of stones with biofilm had a slope close to the reference: their thermal behaviour became homogeneous thanks to biofilm. Indeed, biofilm settled at the stone surface filled pores and therefore decreased air amount inside. Biofilm and limestone effusivity seemed close to each other.

In damp condition, the control stones regression line deviated less from the reference than in dry condition. b_{water} is 1588 $J.K^{-1}.m^{-2}.s^{-1/2}$ which is close to $b_{limestone}$. Water inside pores induced a thermal behaviour closer to a homogeneous material than in dry condition. Moreover, biofilm favoured the thermal homogeneity of the stone due to the moisture content inside it (Schmitt & Flemming, 1999).

Conclusion

The IRT is extensively used for building diagnostics with the concerns of the heat energy loss and the cost savings. This study is the first lab experiment using IRT with the aim of defining this technique ability to detect early stages of biofilms on stone before its visual staining. Analysis of temperature displayed that the heating was higher on the stone surface with biofilm than without it in dry and damp conditions. IRT detected thermal variations on stones due to the biofilm settlement. Variations were most significant in dry condition: stones with biofilm had the highest heating and the fastest cooling time. In addition, dry Savonnieres stones appeared not to be a homogeneous material due to air within the significant open porosity. Biofilm filled partially pores which decreased discontinuities on the surface and changed the stone response to a flash pulse. Such results encouraged to go further in the study on various stones of different intrinsic properties to refine the involvement of biofilm on the change of thermal response.

Acknowledgements

The authors wish to thank M. Marlat, Director of the residential school Sacré Coeur in Reims city for the authorization to set up the outdoor station in the grounds of the secondary school.

References

Ahmed, E., & Holmström, S. J. M. (2015). Microbe–mineral interactions: The impact of surface attachment on mineral weathering and element selectivity by microorganisms. *Chemical Geology*, *403*, 13–23. https://doi.org/10.1016/j.chemgeo.2015.03.009

Avdelidis, N. P., & Moropoulou, A. (2004). Applications of infrared thermography for the investigation of historic structures. *Journal of Cultural Heritage*, *5*(1), 119–127. https://doi.org/10.1016/j.culher.2003.07.002

Avdelidis, N. P., Moropoulou, A., & Theoulakis, P. (2003). Detection of water deposits and movement in porous materials by infrared imaging. *Infrared Physics & Technology*, *44*(3), 183–190. https://doi.org/10.1016/S1350-4495(02)00212-8

Barreira, E., & Almeida, R. M. S. F. (2015). Drying Evaluation Using Infrared Thermography. *Energy Procedia*, *78*, 170–175. https://doi.org/10.1016/j.egypro.2015.11.135

Becerra, J., Ortiz, P., Zaderenko, A. P., & Karapanagiotis, I. (2020). Assessment of nanoparticles/nanocomposites to inhibit micro-algal fouling on limestone façades. *Building Research & Information*, *48*(2), 180–190. https://doi.org/10.1080/09613218.2019.1609233

Beck, J. V., Cole, K. D., Haji-Sheikh, A., & Litkouhl, B. (1992). *Heat conduction using Green's function*. Taylor & Francis.

Bodnar, J. L., Candoré, J. C., Nicolas, J. L., Szatanik, G., Detalle, V., & Vallet, J. M. (2012). Stimulated infrared thermography applied to help restoring mural paintings. *NDT & E International*, *49*, 40–46. https://doi.org/10.1016/j.ndteint.2012.03.007

Borderie, F., Tête, N., Cailhol, D., Alaoui-Sehmer, L., Bousta, F., Rieffel, D., Aleya, L., & Alaoui-Sossé, B. (2014). Factors driving epilithic algal colonization in show caves and new insights into combating biofilm development with UV-C treatments. *Science of the Total Environment*, *484*(1), 43–52. Scopus. https://doi.org/10.1016/j.scitotenv.2014.03.043

Carlomagno, G. M., & de Luca, L. (1987). Heat transfer measurements by means of infrared thermography. *Flow Visualization IV*, 611.

Cutler, N. A., Viles, H. A., Ahmad, S., McCabe, S., & Smith, B. J. (2013). Algal 'greening' and the conservation of stone heritage structures. *Science of The Total Environment*, *442*, 152–164. https://doi.org/10.1016/j.scitotenv.2012.10.050

De los Rios, A., & Ascaso, C. (2005). Contributions of in situ microscopy to the current understanding of stone biodeterioration. *International Microbiology*, *8*(3), 181.

De Vriendt, A. B. (1998). *La Transmission de la chaleur: Introduction au rayonnement thermique* (Vol. 2). G. Morin.

Di Martino, P. (2016). What About Biofilms on the Surface of Stone Monuments? *The Open Conference Proceedings Journal*, *7*(1). https://doi.org/10.2174/2210289201607020014

European commitee for Standardization. (2008). *CSN EN ISO 11664-4 - Colorimetry - Part 4: CIE 1976 L*a*b* Colour space (ISO 11664- 4:2008), Category: 0117 Optics*. Https://Www.En-Standard.Eu. https://www.en-standard.eu/csn-en-iso-11664-4-colorimetry-part-4-cie-1976-l-a-b-colour-space-iso-11664-4-2008/

European Commitee for Standardization. (2010). *NF EN 15801 - Conservation of cultural property – test methods – determination of water absorption by capillarity*. https://www.boutique.afnor.org/norme/nf-en-15801/conservation-des-biens-culturels-methodes-d-essai-determination-de-l-absorption-par-capillarite/article/644915/fa155138

Eyssautier-Chuine, S., Gommeaux, M., Moreau, C., Thomachot-Schneider, C., Fronteau, G., Pleck, J., & Kartheuser, B. (2014). Assessment of new protective treatments for porous limestone combining water-repellency and anti-colonization properties. *Quarterly Journal of Engineering Geology and Hydrogeology*, *47*(2), 177–187. https://doi.org/10.1144/qjegh2013-026

Gambino, M., Sanmartín, P., Longoni, M., Villa, F., Mitchell, R., & Cappitelli, F. (2019). Surface colour: An overlooked aspect in the study of cyanobacterial biofilm formation. *Science of The Total Environment*, *659*, 342–353. https://doi.org/10.1016/j.scitotenv.2018.12.358

Garty, J. (1990). Influence of epilithic microorganisms on the surface temperature of building walls. *Canadian Journal of Botany*, *68*(6), 1349–1353. https://doi.org/10.1139/b90-171

Gavrilov, D., Maev, R. Gr., & Almond, D. P. (2014). A review of imaging methods in analysis of works of art: Thermographic imaging method in art analysis. *Canadian Journal of Physics*, *92*(4), 341–364. Scopus. https://doi.org/10.1139/cjp-2013-0128

Goffredo, G. B., Accoroni, S., Totti, C., Romagnoli, T., Valentini, L., & Munafò, P. (2017). Titanium dioxide based nanotreatments to inhibit microalgal fouling on building stone surfaces. *Building and Environment*, *112*, 209–222. https://doi.org/10.1016/j.buildenv.2016.11.034

Grossi, C. M., & Brimblecombe, P. (2008). Past and future colouring patterns of historic stone buildings. *Materiales de Construcción*, *58*(289–290), 143–160. https://doi.org/10.3989/mc.2008.v58.i289-290.81

Grossi, C. M., Brimblecombe, P., Esbert, R. M., & Alonso, F. J. (2007). Color changes in architectural limestones from pollution and cleaning. *Color Research & Application*, *32*(4), 320–331. https://doi.org/10.1002/col.20322

Hirsch, P., Eckhardt, F. E. W., & Palmer, R. J. (1995). Methods for the study of rock-inhabiting microorganisms—A mini review. *Journal of Microbiological Methods*, *23*(2), 143–167. https://doi.org/10.1016/0167-7012(95)00017-F

Hladik, J. (1997). *Métrologie des propriétés thermophysiques des matériaux*. http://archives.umc.edu.dz/handle/123456789/118975

Jaeger, J. C., & Carslaw, H. S. (1959). *Conduction of heat in solids*. Clarendon P.

Kluge, B., Peters, A., Krüger, J., & Wessolek, G. (2013). Detection of soil microbial activity by infrared thermography (IRT). *Soil Biology and Biochemistry*, *57*, 383–389. Scopus. https://doi.org/10.1016/j.soilbio.2012.09.022

Kylili, A., Fokaides, P. A., Christou, P., & Kalogirou, S. A. (2014). Infrared thermography (IRT) applications for building diagnostics: A review. *Applied Energy*, *134*, 531–549. https://doi.org/10.1016/j.apenergy.2014.08.005

Li, X., Arai, H., Shimoda, I., Kuraishi, H., & Katayama, Y. (2008). Enumeration of Sulfur-Oxidizing Microorganisms on Deteriorating Stone of the Angkor Monuments, Cambodia. *Microbes and Environments*, *23*(4), 293–298. https://doi.org/10.1264/jsme2.ME08521

Maldague, X. (2001). *Theory and practice of infrared technology for nondestructive testing*. Wiley.

McNamara, C. J., & Mitchell, R. (2005). Microbial deterioration of historic stone. *Frontiers in Ecology and the Environment*, *3*(8), 445–451. https://doi.org/10.1890/1540-9295(2005)003[0445:MDOHS]2.0.CO;2

Mihajlovski, A., Seyer, D., Benamara, H., Bousta, F., & Di Martino, P. (2014). An overview of techniques for the characterization and quantification of microbial colonization on stone monuments. *Annals of Clinical Microbiology and Antimicrobials*, http://link.springer.com/article/10.1007%2Fs13213-014-0956-2. https://doi.org/10.1007/s13213-014-0956-2

Moropoulou, A., Avdelidis, N. P., Karoglou, M., Delegou, E. T., Alexakis, E., & Keramidas, V. (2018). Multispectral applications of infrared thermography in the diagnosis and protection of built cultural heritage. *Applied Sciences (Switzerland)*, *8*(2). Scopus. https://doi.org/10.3390/app8020284

Moropoulou, A., Karoglou, M., Bakolas, A., Krokida, M., & Maroulis, Z. B. (2014). Moisture Transfer Kinetics in Building Materials and Components: Modeling, Experimental Data, Simulation. In J. M. P. Q. Delgado (Ed.), *Drying and Wetting of Building Materials and Components* (pp. 27–49). Springer International Publishing. https://doi.org/10.1007/978-3-319-04531-3_2

Moropoulou, A., Labropoulos, K. C., Delegou, E. T., Karoglou, M., & Bakolas, A. (2013). Non-destructive techniques as a tool for the protection of built cultural heritage. *Construction and Building Materials*, *48*, 1222–1239. https://doi.org/10.1016/j.conbuildmat.2013.03.044

Mouhoubi, K. (2016). *Thermographie infrarouge stimulée appliquée à la détection et à la caractérisation d'altérations structurales de peintures murales du patrimoine.* [Reims champagne Ardenne]. http://www.theses.fr/2016REIMS001

Nuhoglu, Y., Oguz, E., Uslu, H., Ozbek, A., Ipekoglu, B., Ocak, I., & Hasenekoglu, I. (2006). The accelerating effects of the microorganisms on biodeterioration of stone monuments under air pollution and continental-cold climatic conditions in Erzurum, Turkey. *Science of the Total Environment*, *364*(1–3), 272–283. Scopus. https://doi.org/10.1016/j.scitotenv.2005.06.034

Özışık, M. N. (1993). *Heat Conduction*. John Wiley & Sons.

Papida, S., Murphy, W., & May, E. (2000). Enhancement of physical weathering of building stones by microbial populations. *International Biodeterioration & Biodegradation*, *46*(4), 305–317. https://doi.org/10.1016/S0964-8305(00)00102-5

Pinheiro, A. Catarina., Mesquita, N., Trovão, J., Soares, F., Tiago, I., Coelho, C., de Carvalho, H. P., Gil, F., Catarino, L., Piñar, G., & Portugal, A. (2018). Limestone biodeterioration: A review on the Portuguese cultural heritage scenario. *Journal of Cultural Heritage*. https://doi.org/10.1016/j.culher.2018.07.008

Pozo-Antonio, J. S., Montojo, C., López de Silanes, M. E., de Rosario, I., & Rivas, T. (2017). In situ evaluation by colour spectrophotometry of cleaning and protective treatments in granitic Cultural Heritage. *International Biodeterioration & Biodegradation*, *123*, 251–261. https://doi.org/10.1016/j.ibiod.2017.07.004

Santunione, G., Ferrari, C., Siligardi, C., Muscio, A., & Sgarbi, E. (2019). Accelerated biological ageing of solar reflective and aesthetically relevant building materials. *Advances in Building Energy Research*, *13*(2), 264–281. https://doi.org/10.1080/17512549.2018.1488616

Schmitt, J., & Flemming, H.-C. (1999). Water binding in biofilms. *Water Science and Technology*, *39*(7), 77–82. https://doi.org/10.1016/S0273-1223(99)00153-5

Tran, T. H., Govin, A., Guyonnet, R., Grosseau, P., Lors, C., Damidot, D., Deves, O., & Ruot, B. (2014). Influence of the intrinsic characteristics of mortars on their biofouling by pigmented organisms: Comparison between laboratory and field-scale experiments. *International Biodeterioration & Biodegradation*, *86*, 334–342. https://doi.org/10.1016/j.ibiod.2013.10.005

Vartoukian, S. R., Palmer, R. M., & Wade, W. G. (2010). Strategies for culture of "unculturable" bacteria. *FEMS Microbiology Letters*, *309*(1), 1–7. Scopus. https://doi.org/10.1111/j.1574-6968.2010.02000.x

Vavilov, V. P., & Maldague, X. P. (1992). Dynamic thermal tomography: new promise in the IR thermography of solids. *Thermosense XIV: An Intl Conf on Thermal Sensing and Imaging Diagnostic Applications*, *1682*, 194–206.

Warscheid, Th., & Braams, J. (2000). Biodeterioration of stone: a review. *International Biodeterioration & Biodegradation*, *46*(4), 343–368. https://doi.org/10.1016/S0964-8305(00)00109-8

Zhang, F., Zhang, X., Li, Y., Tao, Z., Liu, W., & He, M. (2018). Quantitative description theory of water migration in rock sites based on infrared radiation temperature. *Engineering Geology*, *241*, 64–75. https://doi.org/10.1016/j.enggeo.2018.05.006